International Journal of Heat and Mass Transfer 52 (2009) 4604–4611

Contents lists available at ScienceDirect

International Journal of Heat and Mass Transfer

journal homepage: www.elsevier.com/locate/ijhmt

A boundary element approach for topology design in diffusive problems containing heat sources

Carla T.M. Anflor, Rogério J. Marczak *

Departamento de Engenharia Mecânica, Universidade Federal do Rio Grande do Sul, Rua Sarmento Leite 425, 90050-170 Porto Alegre, RS, Brazil

ARTICLE INFO

Article history:
Received 6 October 2006
Accepted 25 February 2009
Available online 21 May 2009

Keywords:
Topology optimization
Heat transfer
Poisson equation
Topological derivative
Orthotropic materials
Boundary element methods

ABSTRACT

The objective of this work is to present the application of a hard-kill material removal algorithm for topology optimization of heat transfer problems containing localized sources. The boundary element method is used to solve the governing equations. A topological-shape sensitivity approach is used to select the points showing the lowest sensitivities, where material is removed by opening a cavity. As the iterative process evolutes, the original domain has holes progressively punched out, until a given stop criteria is achieved. Both isotropic and orthotropic two-dimensional benchmarks are presented and analyzed. Because the BEM does not employ domain meshes in linear cases, the resulting topologies are completely devoid of intermediary material densities. Although the drawbacks of hard-kill methods are still present, the approach opens an interesting field of investigation for integral equation methods.

1. Introduction

Most of the research on shape and topology optimization carried out during the last decade has been focused on elasticity problems [2]. The thermal conducting solid issue has received relatively less attention in spite of its significance for industrial applications such as polymer curing in die-molding processes, printed circuit board designs, and heat diffusers, to cite a few. Among the numerical techniques developed for topology optimization, SIMP (solid isotropic material with penalization) and ESO (evolutionary structural optimization) rank as the dominant methods, and both (along with their variants) have been successfully used in many optimization fields (a recent comprehensive review can be found in [13]. Both families have advantages and disadvantages, but the need of handling and controlling intermediary material densities plays an important role in SIMP methods. A natural consequence of the use of variable material densities is the choice of the finite element method (FEM) for the numerical solution of the governing equations. Additionally, the technique is able to generate globally optimal solutions, i.e., microstrutured designs. Although strictly correct from the mathematical standpoint, this type of solution often fails to generate engineering designs directly. In order to render a 0–1 (void-material) solution, suboptimal microstructures with penalization of the density gradient are used to avoid large areas with intermediate material, in some cases leading to numerical instabilities.

Topological derivative (TD) or topological-shape sensitivity methods [21,5,3,4] are a family of ESO methods based on unidirectional (hard-kill) or bidirectional material removal/addition. Essentially, TD methods aim to remove material where it is less necessary after a suitable cost function. The main advantage of TD methods lies in the use of a constant density, rendering fully 0–1 design solutions. Since the methodology shares the well known disadvantages of any hard-kill method, it may lead to non-optimal solutions unless some fine tuning is incorporated to the iterative process. However, it performs very well in highly convex problems, like steady state linear potential problems, elastic torsion, and electrostatic problems.

The fact that the boundary element method (BEM) can deliver very efficient predictions with relatively coarse meshes (in comparison to other methods like the FEM) can be used to reduce significantly the computational cost of highly iterative processes like optimization, particularly in shape optimization. Much of that advantage is, however, lost in topology optimization applications due to the need of sensitivity evaluation at internal points.

So far, the BEM has been used mostly for shape optimization problems. Marczak [14] introduced the application of a TD method using the BEM applied to the optimization of linear isotropic potential problems. Since the BEM does not need domain mesh, its use with TD methods renders a fully 0–1 approach, thus avoiding intermediary material densities and the associated numerical drawbacks, such as checkerboard instability [2]. One of the objectives of the present work is to extend the method to solids with orthotropic behavior. The other goal relies in verifying the topologies obtained when multiple localized heat sources are present in the domain.

* Corresponding author.
E-mail address: rato@mecanica.ufrgs.br (R.J. Marczak).

0017-9310/$ - see front matter © 2009 Elsevier Ltd. All rights reserved.
doi:10.1016/j.ijheatmasstransfer.2009.02.048

In the present work, the TD formulation focused on isotropic potential equation is reviewed. The conformal mapping technique is also revisited, aiming the numerical solution of anisotropic problems by modifying a standard BEM code developed for the isotropic case. A numerical methodology is devised to carry out the computational design by an iterative BEM procedure. A number of linear heat transfer examples are solved with the proposed formulation and the results are compared with those available in the literature.

2. Review of topological derivative

A topological derivative formulation for Poisson Equation is used throughout this work [4,15]. The original concept is related to the sensitivity of a given cost function $\psi(\Omega)$ (total potential energy, in the present case) when the topology of the original analysis domain Ω is changed. Therefore, after opening a hole of small radius (ε) at a point $\hat{x}$ inside the design domain, the cost function changes to $\psi(\Omega_\varepsilon)$, and the sensitivity can be evaluated by:

$$D_T^*(\hat{x}) = \lim_{\varepsilon \to 0} \frac{\psi(\Omega_\varepsilon) - \psi(\Omega)}{f(\varepsilon)} \tag{1}$$

where $\psi(\Omega)$ and $\psi(\Omega_\varepsilon)$ are the cost functions evaluated on the original and on the perturbed domains, respectively, and f is a regularizing function. Eq. (1) does not allow to establish a direct isomorphism between the domains Ω and Ω_ε, since they have different topologies. Feijóo et al. [4] modified Eq. (1) applying the idea that the creation of hole can be accomplished by perturbing an existing one whose radius tends to zero. In this case, it becomes easier to establish a mapping between both domains, i.e., one containing a hole and another containing a perturbed hole (Fig. 1). The topological derivative definition in this case reads [15]:

$$D_T(\hat{x}) = \lim_{\varepsilon \to 0} \frac{\psi(\Omega_{\varepsilon+\delta\varepsilon}) - \psi(\Omega_\varepsilon)}{f(\Omega_{\varepsilon+\delta\varepsilon}) - f(\Omega\varepsilon)} \tag{2}$$

where $\delta\varepsilon$ is a perturbation on the hole's radius.

In the case of isotropic linear heat transfer problems, the direct problem is stated as:

$$\text{Solve}\{u_\varepsilon | -k\Delta u_\varepsilon = b\} \quad \text{on} \quad \Omega_\varepsilon \tag{3}$$

$$\text{subjected to} \begin{cases} u_\varepsilon = \overline{u} & \text{on} \quad \Gamma_D \\ k\frac{u}{n} = \overline{q} & \text{on} \quad \Gamma_N \\ k\frac{u_\varepsilon}{n} = h_c(u_\varepsilon - u_\infty) & \text{on} \quad \Gamma_R \end{cases} \tag{4}$$

and to

$$h(\alpha, \beta, \gamma) = 0 \text{ on } \Gamma_\varepsilon$$

where Γ_ε stands for the holes boundary and

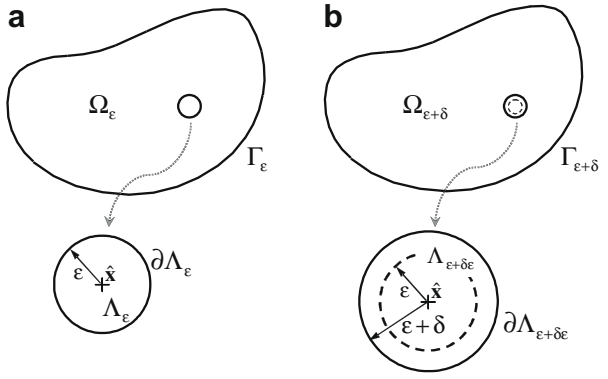

Fig. 1. Modified concept of topological sensitivity. (a) Original domain Ω_ε. (b) Perturbed domain $\Omega_{\varepsilon+\delta\varepsilon}$.

Table 1
Analytical expressions for topological derivatives in Poisson problems.

b.c. Type	$D_T(\hat{x})$	$\hat{x}$
Neumann ($\alpha = 0$, $\beta = 1$, $\gamma = 0$)	$D_T(\hat{x}) = k\nabla u \nabla u - bu$	$\hat{x} \in \Omega \cup \Gamma$
	$D_T(\hat{x}) = -q_\varepsilon u$	$\hat{x} \in \Omega \cup \Gamma$
Robin ($\alpha = 1$, $\beta = 0$, $\gamma = 0$)	$D_T(\hat{x}) = h_c^\varepsilon(u_\varepsilon - 2u_{\varepsilon\infty})$	$\hat{x} \in \Omega \cup \Gamma$
Dirichlet ($\alpha = 1$, $\beta = 0$, $\gamma = 0$)	$D_T(\hat{x}) = -\frac{1}{2}k(u - \overline{u}_\varepsilon)$	$\hat{x} \in \Omega$
	$D_T(\hat{x}) = k\nabla u \nabla u - b\overline{u}_\varepsilon$	$\hat{x} \in \Gamma$

$$h(\alpha,\beta,\gamma) = \underbrace{\alpha(u_\varepsilon - \overline{u}^\varepsilon)}_{\text{Dirichlet}} + \underbrace{\beta\left(k\frac{\partial u_\varepsilon}{\partial n} + \overline{q}^\varepsilon\right)}_{\text{Neumann}} + \underbrace{\gamma\left(k\frac{\partial u_\varepsilon}{\partial n} + h_c^\varepsilon(u_\varepsilon - u_\infty^\varepsilon)\right)}_{\text{Robin}} = 0 \tag{5}$$

is a function which takes into account the type of boundary condition on the perimeter of holes to be created. In Eq. (5), u_ε and $\delta_{u_\varepsilon}/\partial_n = q_\varepsilon$ are the temperature and the flux on the hole boundary, while u_∞^ε and h_c^ε are the hole's internal convection parameters, respectively. Suitable choices of α, β and γ define the type of boundary condition on the hole.

Using asymptotic expansions to include the effects of a hole inserted in Ω it is possible derive analytic expressions for and $\psi(\Omega_{\varepsilon+\delta\varepsilon})$, which are used to generate the final expressions for Eq. (2). Further details can be found in [15].

After an intensive analytical work, Feijóo et al. [4] have developed these expressions in problems governed by Eq. (3), taking the total potential energy as a cost function. The main results are reproduced in Table 1, considering the three classical cases of boundary conditions on the holes.

3. Numerical methodology

Since Eq. (3) and its $D_T(\hat{x})$ counterparts of Table 1 are valid only for isotropic domains, conformal mapping techniques can be used to reduce a steady state anisotropic field to an isotropic equivalent. The advantage of this method relies in the fact that the coordinate directions of the mapped domain remain straight. The method is very well known and has been applied along with numerical methods like the FEM and the BEM before. Poon [17] investigated the heat conduction problems in layered composites with orthotropic materials, while Poon et al. [16] extended the work for anisotropic media. Shiah and Tan [18] applied the coordinate transformation to map an initial anisotropic heat transfer field to an equivalent isotropic domain using the BEM. Hsieh and Ma [6] introduced a linear coordinate transformation method to solve heat conduction on a thin layer of anisotropic medium subjected to arbitrary thermal loadings applied inside the domain or on the boundary surfaces. Ma and Chang [12] studied two-dimensional steady-state thermal conduction problems on anisotropic multi-layered media. They have used the linear coordinate transformation to simplify the governing equation without complicating the boundary and interface conditions. Shiah and Tan [19] extended their earlier work [18] to three-dimensional anisotropic field problems.

The differential equation for anisotropic two-dimensional heat conduction in a Cartesian coordinate system [1] is given by:

$$k_{xx}\frac{\partial^2 T}{\partial x^2} + 2k_{xy}\frac{\partial^2 T}{\partial x \partial y} + k_{yy}\frac{\partial^2 T}{\partial y^2} = 0 \tag{6}$$

where k_{xx}, k_{yy} and k_{xy} are the thermal conductivity coefficients, while T represents the temperature field. The corresponding heat fluxes are expressed as:

$$\begin{aligned} q_x &= -k_{xx}\frac{\partial T}{\partial x} - k_{xx}\frac{\partial T}{\partial y} \\ q_y &= -k_{xy}\frac{\partial T}{\partial x} - k_{yy}\frac{\partial T}{\partial y} \end{aligned} \tag{7}$$

The following linear coordinate transformation is used [17]:

$$\begin{bmatrix}\hat{x}\\ \hat{y}\end{bmatrix}=\begin{bmatrix}1 & \alpha\\ 0 & \beta\end{bmatrix}\begin{bmatrix}x\\ y\end{bmatrix} \tag{8}$$

where $\alpha = -k_{xy}/k_{yy}$, $\beta = k/k_{yy}$, and $k=\sqrt{k_{xx}k_{yy}-k_{xy}^2}$. Now the governing equation in the transformed domain reads:

$$k\left(\frac{\partial^2 T}{\partial \hat{x}^2}+\frac{\partial^2 T}{\partial \hat{y}^2}\right)=0 \tag{9}$$

where k is the equivalent thermal conductivity. Eq. (9) now resembles Eq. (3), i.e., an equivalent isotropic problem. It is interesting to point out that when, $K_{xy} = 0$ the transformation of Eq. (8) is merely a rotation of the constitutive coordinate system to its principal directions. Neumann boundary conditions also must be transformed accordingly:

$$\begin{aligned} q_y &= -k\frac{\partial T}{\partial y}=q_{\hat{y}}\\ q_x &= \beta q_{\hat{x}}-\alpha q_{\hat{y}}\end{aligned} \tag{10}$$

By inverting the Eq. (10), the Neumann boundary conditions are promptly recovered as a function of the original domain boundary conditions.

$$\begin{aligned} q_{\hat{y}} &= q_y\\ q_{\hat{x}} &= \frac{q_x+\alpha q_y}{\beta}\end{aligned} \tag{11}$$

In the present work, the boundary element method was used as numerical method to solve the governing equations. The boundary integral equation for problems governed by Eq. (3) is given by [9]:

$$c(\hat{x})T(\hat{x})+\int_\Gamma q^*(\hat{x},\hat{y})T(\hat{y})d\Gamma=\int_\Gamma T^*(\hat{x},\hat{y})q(\hat{y})d\Gamma+\int_\Omega T^*(\hat{x},\hat{y})b(\hat{y})d\Gamma \tag{12}$$

where c is the geometric factor of the boundary point $\hat{x}$, T and q are the temperatures and the fluxes on the boundary Γ, respectively, and b is the heat generated inside the domain Ω. The symbols T^* and q^* refer to the temperature and flux fundamental solutions for an infinite medium:

$$T^*(\hat{x},\hat{y})=\frac{-1}{2\pi kt}\ln(\hat{x}-\hat{y}) \tag{13}$$

$$q^*(\hat{x},\hat{y})=-k\nabla T^*(\hat{x},\hat{y})\cdot\mathbf{n}(\hat{y}) \tag{14}$$

where t is the thickness of the medium and $\mathbf{n}$ is the outward normal of the boundary Γ at $\hat{y}$. In the cases where there are n heat sources of intensity s inside the domain, placed at coordinates $\hat{z}$, the last term of Eq. (12) can be particularized by replacing b for a concentrated heat source [8]:

$$b(\hat{y})=\sum_{i=1}^{n}s(\hat{z}_i)\delta(\hat{y},\hat{z}_i) \tag{15}$$

and Eq. (12) is rewritten as:

$$c(\hat{x})T(\hat{x})+\int_\Gamma q^*(\hat{x},\hat{y})T(\hat{y})d\Gamma=\int_\Gamma T^*(\hat{x},\hat{y})q(\hat{y})d\Gamma+\sum_{i=1}^{n}T^*(\hat{x},\hat{z})s(\hat{z}_i) \tag{16}$$

where $\hat{x}\in\Gamma$. After the usual discretization of the boundary Γ in boundary elements, and parameterization of the temperature and fluxes through interpolation functions, Eq. (16) is applied to each boundary nodal point $\hat{x}$, generating the system of equations:

$$\mathbf{HT}=\mathbf{GQ}+\mathbf{f} \tag{17}$$

where the vectors $\mathbf{T}$ and $\mathbf{Q}$ contain the temperature and fluxes of the boundary nodes, while the last term on the right side contains the heat sources contribution. Since at each nodal point on Γ whether the temperature or the normal heat flux is known, the columns of Eq. (17) can be exchanged to group the boundary unknowns in a single vector $\mathbf{X}$:

$$\mathbf{AX}=\mathbf{B} \tag{18}$$

Once the system of Eq. (17) is solved, all the boundary variables are known, and the temperature on interior points can be recovered as a post-processing step, using the integral equation for temperatures at internal points [9]:

$$T(\hat{x})=\int_\Gamma T^*(\hat{x},\hat{y})q(\hat{y})d\Gamma-\int_\Gamma q^*(\hat{x},\hat{y})T(\hat{y})d\Gamma+\sum_{i=1}^{n}T^*(\hat{x},\hat{z})s(\hat{z}_i) \tag{19}$$

with $\hat{x}\in\Omega$.

In order to adapt a BEM code based on Eqs. (16) and (19) for topology optimization of orthotropic media, the following algorithm was implemented (see Fig. 1):

Start with the orthotropic domain mesh and a suitable grid of internal points.

Transform an orthotropic domain into an equivalent isotropic one by the linear coordinate transformation given by Eq. (8). The Neumann b.c., the coordinates of internal points and the heat sources inside the domain also must be transformed. Solve the problem by the BEM as an isotropic case, including temperatures and fluxes at internal points.

The topological sensitivities are then evaluated at all interior points by using the formulas from Table 1, according to the desired b.c. The points with the lowest values of D_T are selected.

Apply the inverse mapping. Holes are created by punching out disks of material centered on the previously selected points. Check stopping criteria, rebuilt the mesh and return to step 1, if necessary. When the process is halted, an optimal topology is expected.

The grid of internal points is generated automatically, taking into account the radius of the holes created during each iteration. Different patterns of internal points can be generated, as discussed by Marczak [14]. In addition, the analyst can restrict the grid to the design areas only, reducing significantly the computational overhead. The radius of the holes are taken as a fraction of a reference dimension of the original domain ($r=\lambda l_{\text{ref}}$), where $l_{\text{ref}}=\min(\text{height},\text{width})$ is generally adopted. The current area of the domain (A_f) is checked at the end of each iteration until the target value is achieved ($A_f=\xi A_0$, where A_0 is the initial area).

4. Results

In this section, some examples are presented in order to assess the algorithm developed. All cases refer to linear steady state heat transfer problems containing localized heat sources inside the domain. Data and boundary condition are illustrated in the accompanying figures. The material removal history is illustrated for each case. The iterative process was halted when a target material volume fraction (A_f/A_0, where A_f and A_0 are the final and initial volume, respectively) was achieved, regardless the type of material medium. This provided a simplified criterion to compare the topologies generated for isotropic, orthotropic, and anisotropic media starting from the same design. In all cases, the total potential energy was used as the cost function. Linear discontinuous boundary elements integrated with four Gauss points were used in all cases. Unless specified otherwise, all cases used holes with $\lambda = 0.03$. The results obtained by Li et al. [10,11] and Steven et al.

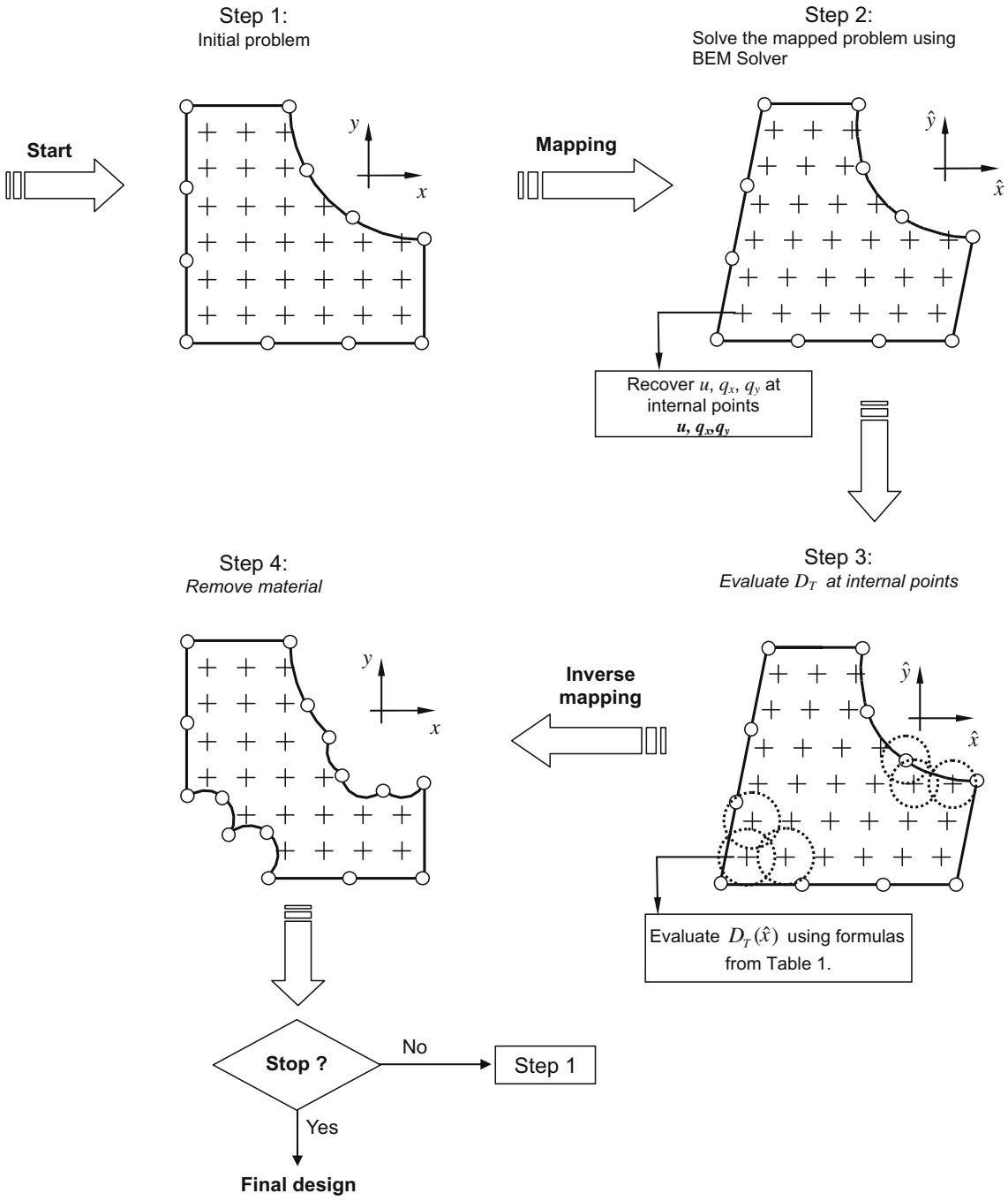

Fig. 2. BEM iterative scheme for material removal.

[20] using the FEM and a weighting factor scheme (WFS) are used for comparison purposes.(See Fig. 2)

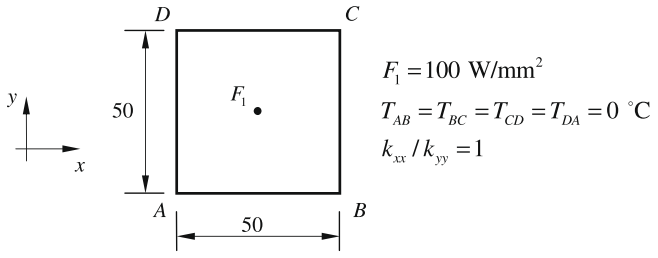

Fig. 3. Square plate with centered heat source.

4.1. Isotropic square plate with a centered heat source

This first case refers to an isotropic square plate with a single centered heat source, which was used to assess the numerical code. The temperature along the boundary (edges *AB*, *BC*, *CD* and *DA*) is maintained at 0 °C. A heat source of 100 W/mm^2 is placed at the plate center (see Fig. 3). The holes open during the process had prescribed temperatures set to 0 °C. The initial boundary mesh has 20 elements per side. The process was halted when $A_f = 0.75A_0$.

Fig. 4 shows the topology evolution obtained for this case, clearly evidencing the tendency to remove material from the corners, leading to a circular shape, as expected due to the radial heat diffusion.

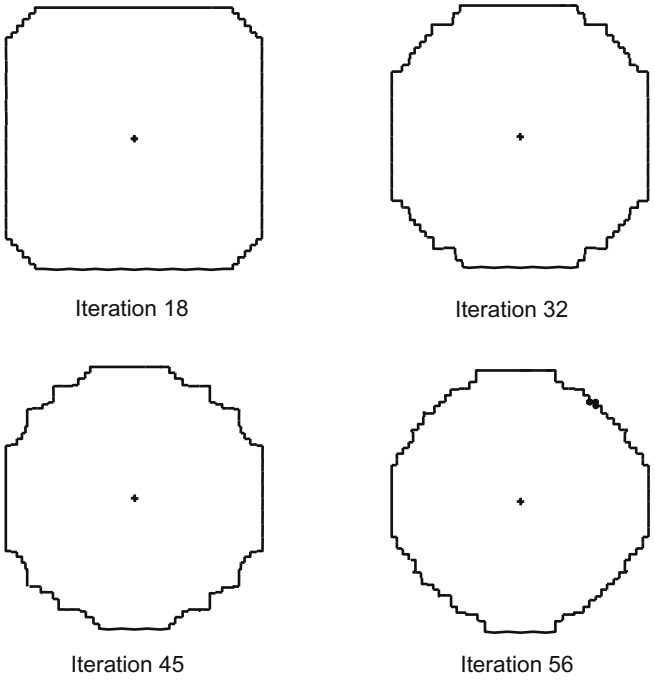

Fig. 4. Topology evolution for the isotropic square plate.

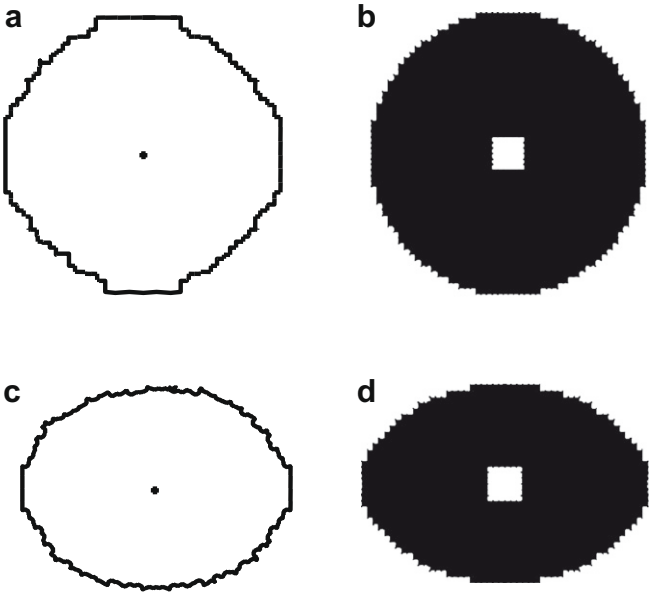

Fig. 6. Comparison of final topologies obtained for square plate with centered heat source: (a) Present result – isotropic ($A_f = 0.75A_0$); (b) Li et al. [10] – isotropic ($A_f = 0.79A_0$); (c) Present result – orthotropic ($A_f = 0.50A_0$); (d) Li et al. [10] – orthotropic ($A_f = 0.47A_0$).

4.2. Orthotropic square plate with a centered heat source

This case has the same geometry and boundary conditions of the previous one, but the constitutive properties are such that $k_{xx}/k_{yy} = 2$. Fig. 5 presents the topology history obtained, eventually resulting an elliptical shape, being the semi-axis in the x direction longer than in the y direction, as expected. The final design corresponds to $A_f = 0.5A_0$. Fig. 6 compares the final topology obtained by the present method with those obtained by Li et al. [10] using the finite element method (FEM) and a weighting factor scheme (WFS).

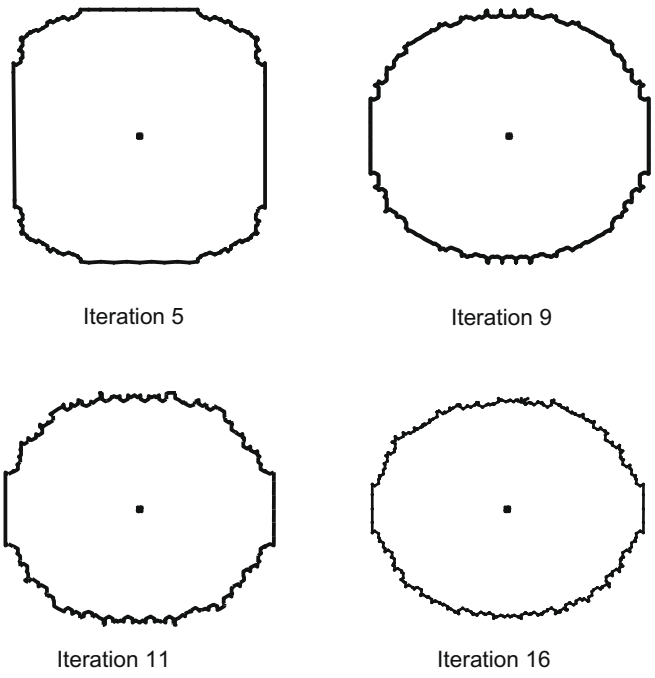

Fig. 5. Topology evolution for the orthotropic square plate.

In the results of Li et al. [10], a square cavity with prescribed temperature was adopted instead of a point source, due to implementational issues. Good agreement of the present results can be observed. Fig. 7 compares the material removal evolution for both, isotropic and orthotropic cases.

4.3. Isotropic rectangular plate with two heat sources

This case can be used to verify the interaction of more than one heat sources acting in the domain. A rectangular plate with dimensions 30×50 mm is excited by two heat sources symmetrically place along the horizontal symmetry line (Fig. 8). All edges have prescribed temperature of 0 °C, as well as the cavities open during the process. Both heat sources are set to 100 W/mm^2. The process was halted when $A_f = 0.5A_0$.

Fig. 9 shows the topology evolution obtained, while Fig. 10 compares the present results with the ones obtained by Li et al. [10]. The agreement between both designs is evident. An additional assess-

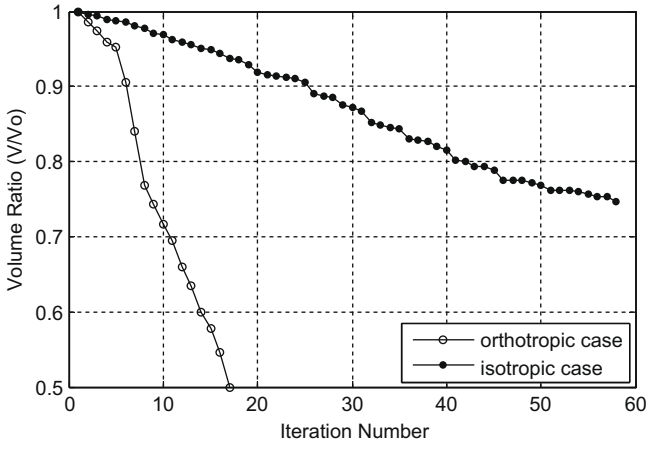

Fig. 7. Evolution history of volume vs. iteration.

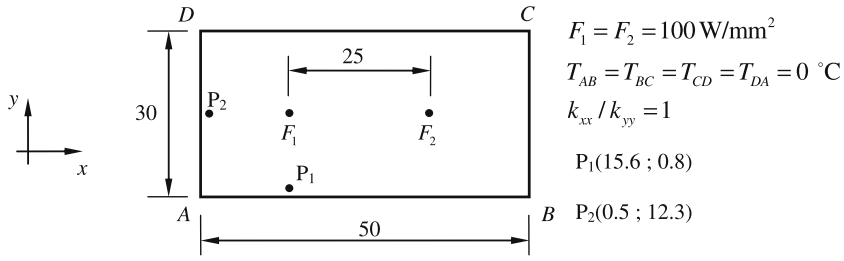

Fig. 8. Isotropic rectangular plate.

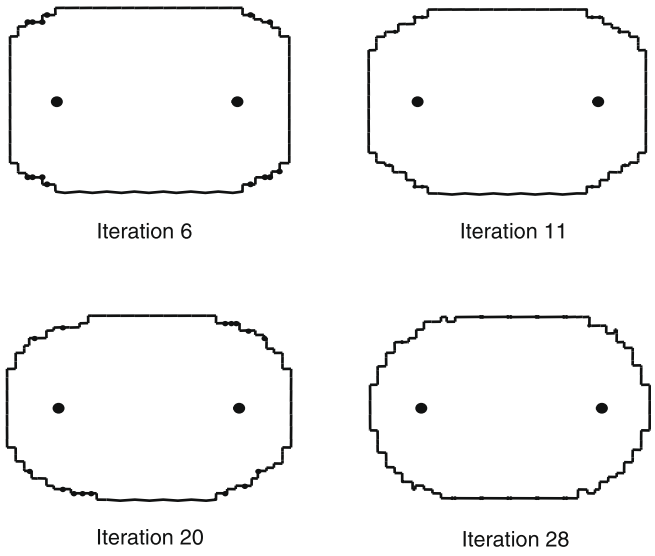

Fig. 9. Topology evolution for isotropic rectangular plate.

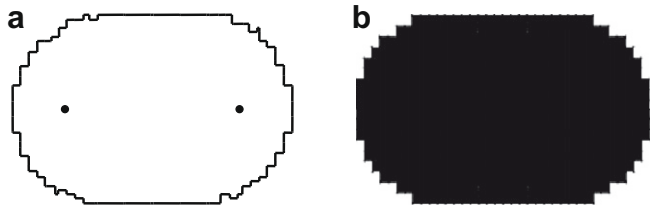

Fig. 10. Final topologies for isotropic rectangular plate: (a) Present result – $A_f = 0.49A_0$; (b) Li et al. [10] – $A_f = 0.47A_0$.

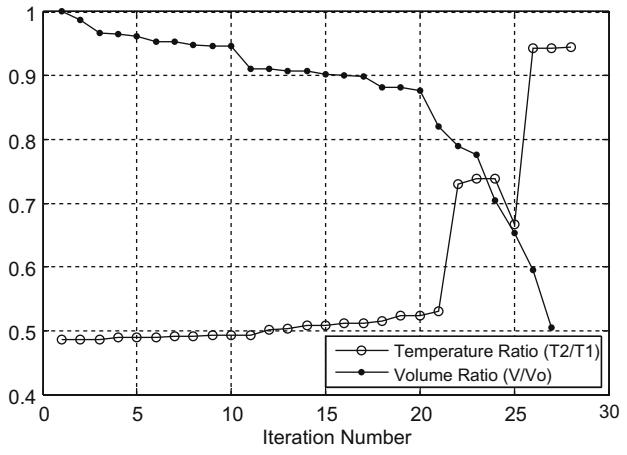

Fig. 11. Evolution history of temperature ratio and volume ratio.

ment of these results can be seen in Fig. 11, where the temperature ratio T_2/T_1 of points $P_1(15.6, 0.8)$ and $P_2(0.5, 12.3)$ (see Fig. 8), is tracked during the iterative process. Since both points are at the same distances from the heat sources, it is clear that the temperature distribution becomes uniform in the optimized design.

4.4. Printed circuit board (PCB)

This example was proposed by Li et al. [10] and refers to a printed circuit board (PCB) substrate. An important aspect of good PCB designs is the ability to dissipate the maximum amount of thermal energy with the minimum possible volume of material. Topology optimization is a valuable tool in such cases, allowing material savings unfeasible using only intuitive design ideas. Fig. 12 shows the initial layout for this case, where four heat sources are used to simulate the heat generated by major electronic components mounted on the PCB. Part of the domain can not be changed (hatched areas in Fig. 12). The BEM model used for this case employed an initial mesh of 32 elements linear elements, and the internal points were placed only within the design area. All the cavities used prescribed Neumann homogeneous boundary condition. The process was halted when a volume ratio of 70% between the final and the original designs was achieved.

Fig. 13 shows the topology history. It is worth to note that all previous examples could be solved by pure shape optimization, since the original topology was not changed. In the PCB case, however, new cavities are created during the process, characterizing truly topological changes in the domain. It is also interesting to note the creation of small cavities near the corners of the PCB. The present approach shows good agreement with the results obtained by Li et al. [10], as shown in Fig. 14.

5. Additional comments

The results presented in the previous section shows clearly that, although useful results can be obtained with the proposed methodology, it shares the very same problems of most hard-kill methods. If conveniently controlled, the designs thus obtained are acceptable, but it may be virtually impossible to specify a sufficiently general material removal rule regardless the application. Furthermore, the imposition of contains to the problem is rather complex, since the analytical expressions for D_T have been derived (in the original references) without considering them.

A major issue in the present formulation is related to the relative magnitude of the D_T values as the iterative process evolves. After the first few iterations, the gradient of D_T along the domain becomes very low, since the optimal solution has constant sensitivities. Since some areas of the domain may be more affected by modeling and discretization errors than others, a fine tuning becomes mandatory to avoid material rejection at non-optimal locations. Another issue is related to the (non-mathematical) stopping criteria used. Specified volume fractions are relatively easy to implement. In the present approach, the current volume is

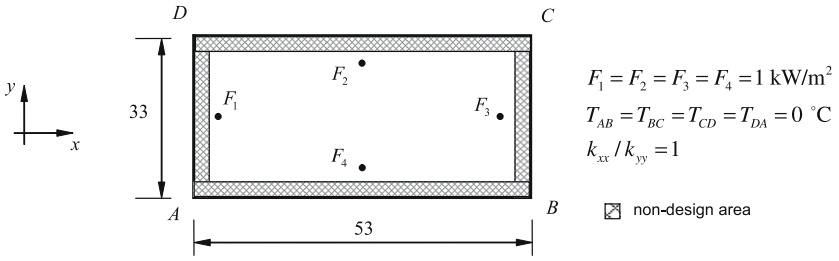

Fig. 12. PCB: initial design.

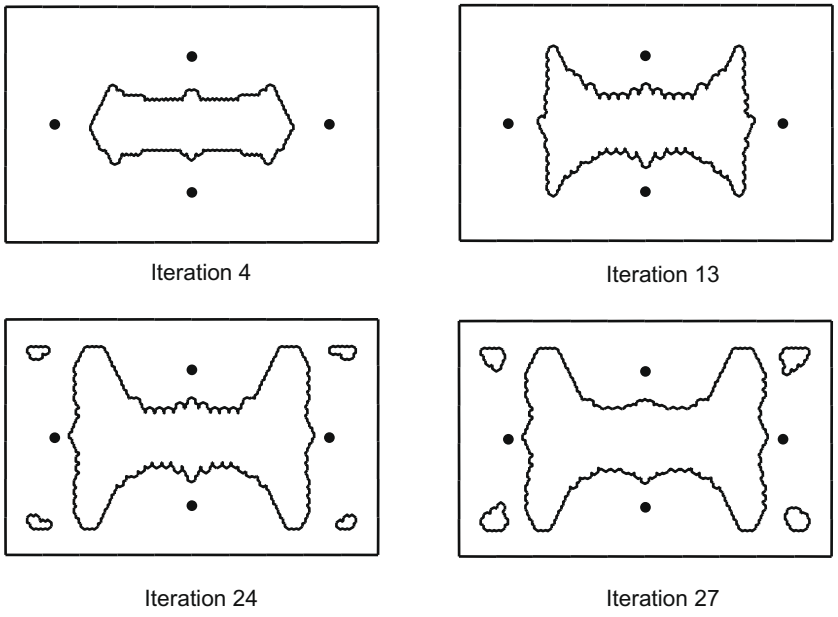

Fig. 13. Topology evolution for the PCB.

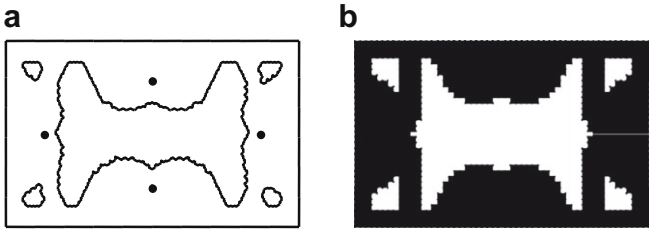

Fig. 14. Final topologies for the PCB: (a) Present results – $A_f = 0.70A_0$; (b) Li et al. [10] – $A_f = 0.68A_0$.

compared with the target volume at the end of each iteration, and the process is halted if necessary (this is possible because the number of holes and the diameters are known during run time). Although useful for material saving, this criteria is devoid of further information like energy content or compliance values.

If, by one side, ESO methods like the one presented here show serious limitations, on the other side one can make interesting usages of D_T, particularly in conjunction with other optimization methods. For instance, if an surface of D_T values is constructed, its isolines could be used to specify a material rejection criteria. The domain obtained after that first iteration can be a good starting point for SIMP methods or a shape optimization analysis. The algorithm used to remove material in the present work leaves something to be desired, delivering unpleasantly jagged boundaries. "Tiling" schemes of material removal [14] has already proved to generate solutions very similar to the ones obtained with SIMP methods, and can be alternatively used. In any case, the smoothness of the resulting boundaries is more related to the size of the holes used to remove material. Regardless the type of hole (circular or squared), the resolution of boundaries generated will be finer when clouds of smaller holes are punched out of the design domain. However, this means a large number of internal points where D_T must be evaluated, increasing the computational cost of the analysis. The ideal situation relies on using holes large enough to accelerate the material removal but yet sufficiently small to capture all relevant geometric features of the optimal design. The sensitivity analysis is not directly affected by the size of the elements, provided the mesh is no too coarse (i.e., providing good results on internal points). The important aspect here is to keep the relative magnitudes of D_T reasonably well estimated along the whole design domain.

Another point to be highlighted here is the possibility of using post-processing algorithms to smooth the boundaries obtained not only with the BEM methodology shown here, but also to eliminate the see-saw aspect of most SIMP approaches reported. Line simplification algorithms encompass a family of tools largely used in cartographic and geographic applications, and can be used to render topology optimization solutions more close to the actual manufacturing designs [22]. Finally, spline-type boundary interpolation can be also used to remove much of the irregularities in the results. Fig. 15 illustrates one of such examples, where the BEM mesh was smoothed by Bézier interpolation.

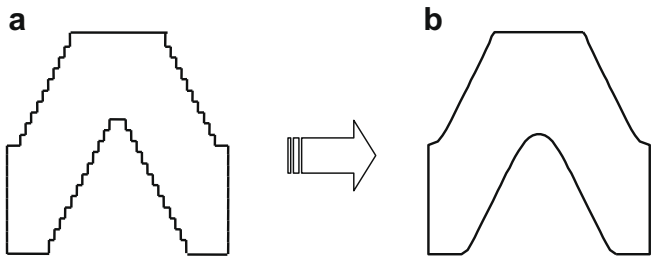

Fig. 15. Example of boundary smoothing. (a) Original result. (b) Beziér-smoothed result.

6. Conclusions

Topology optimization applied to heat transfer problems is still relatively scarce in the literature, when compared to other fields. This scarceness is more evident when the topic is focused on problems considering non-isotropic media. The present work has shown an extension of earlier works to allow the solution of non-isotropic topology optimization problems under a BEM numerical structure. This was accomplished by accommodating a simple linear transformation in the original optimization scheme, allowing the use of topological-shape sensitivities developed for isotropic problems. A methodology for material removal was devised to progressively eliminate material where the sensitivities are low enough. The application of coordinate transformations within a BEM solver thus avoids potential problems associated mesh distortion found in other numerical methods. Therefore, the BEM's characteristic good accuracy for boundary variables (both temperature and heat flux) can be explored to obtain better estimates for topological sensitivities. The effectiveness of the proposed scheme is tested for a number of cases, and the final topologies obtained are compared with other solutions from the literature. Good agreement was found in all cases.

Acknowledgment

Carla T.M. Anflor thanks CNPq for a fellowship grant.

References

[1] V.S. Arpaci, S. Kao, A. Selamet, Introduction to Heat Transfer, Prentice Hall, Upper Saddle River, NJ, 1990.
[2] M.P. Bendsøe, Optimization of Structural Topology, Shape, and Material, Springer-Verlag, Berlin, 1995.
[3] J. Céa, S. Garreau, P. Guillaume, M. Masmoudi, The shape and topological optimizations connection, Comput. Methods Appl. Mech. Eng. 188 (2000) 713–726.
[4] R. Feijóo, A. Novotny, E. Taroco, C. Padra, The topological derivative for the poisson's problem, Math. Mod. Methods Appl. Sci. 13 (2003) 1825–1844.
[5] S. Garreau, P. Guillaume, M. Masmoudi, The topological gradient, Research report, Université Paul Sabatier, Toulouse 3, France, 1998.
[6] M. Hsieh, C. Ma, Analytical investigations for heat conduction problems in anisotropic thin-layer media with embedded heat sources, Int. J. Heat Mass Transfer 45 (2002) 4117–4132.
[8] N. Kamiya, Y. Sawaki, An efficient BEM for some inhomogeneous and nonlinear problems, in: C.A. Brebbia, G. Maier (Eds.), Proc. of the 7th Int. Sem. BEM Eng., vol. 13, Villa Olmo, Italy, 1985, pp. 59–68.
[9] J.H. Kane, Boundary Element Analysis in Engineering Continuum Mechanics, Prentice-Hall, 1994.
[10] Q. Li, G. Steven, O. Querin, Y. Xie, Shape and topology design for heat conduction by evolutionary structural optimization, Int. J. Heat Mass Transfer 42 (1999) 3361–3371.
[11] Q. Li, G. Steven, Y. Xie, O. Querin, Evolutionary topology optimization for temperature reduction of heat conduction fields, Int. J. Heat Mass Transfer 47 (2004) 5071–5083.
[12] C. Ma, S. Chang, Analytical exact solutions of heat conduction problems for anisotropic multi-layered media, Int. J. Heat Mass Transfer 47 (2004) 1643–1655.
[13] J. Mackerle, Topology and shape optimization of structures using FEM and BEM – a bibliography (1999–2001), Finite Elem. Anal. Des. 39 (2003) 243–253.
[14] R.J. Marczak, Topology optimization and boundary elements – a preliminary implementation for linear heat transfer, Eng. Anal. Boundary Elem. 31 (2007) 793–802.
[15] A. Novotny, R. Feijóo, E. Taroco, C. Padra, Topological-shape sensitivity analysis, Comput. Methods Appl. Mech. Eng. 192 (2003) 803–829.
[16] K.C. Poon, R.C.H. Tsou, Y.P. Chang, Solution of anisotropic problems of first class by coordinate-transformation, J. Heat Transfer 101 (1979) 340–345.
[17] K.C. Poon, Transformation of heat conduction problems in layered composites from anisotropic to orthotropic, Lett. Heat Mass Transfer 6 (1979) 503–511.
[18] Y.C. Shiah, C.L. Tan, BEM treatment of two-dimensional anisotropic field problems by direct domain mapping, Eng. Anal. Boundary Elem. 20 (1997) 347–351.
[19] Y.C. Shiah, C.L. Tan, BEM treatment of three-dimensional anisotropic field problems by direct domain mapping, Eng. Anal. Boundary Elem. 28 (2004) 43–52.
[20] G. Steven, Q. Li, Y. Xie, Evolutionary topology and shape design for general physical field problems, Comput. Mech. 26 (2000) 129–139.
[21] J. Sokolowski, A. Zochowski, On topological derivative in shape optimization, Research Report 3170, INRIA-Lorraine, France, 1997.
[22] E.L. Cardoso, R.J. Marczak, Application of genetic algorithms for boundary description in topology optmization solutions, in: Proc. of the XXVII Iberian Latin American Congress on Computational Methods in Engineering, Braz. Assoc. Comput. Mech., 2006.